• Supplementary Material •

Deep Metric Learning for Unsupervised Remote Sensing Change Detection

1. Additional Details on PCC

Polynomial color correction has been originally used in device characterization. In CD, we adopt this concept to map pre-change color space to post-change color space so that resulting difference image $\mathbf{I}_d$ is less sensitive to isolated radiometric changes in pre-change and post-change images. Suppose that, we have N color samples from the post-change image, the corresponding camera response i_1, i_2, i_3, ..., i_b (where b is the total number of color bands) can be represented by a $1 \times b$ vector ρ_n where $n = 1, 2, 3, .., N$. If only i_1, i_2, i_3, ..., i_b values are utilized in ρ_n, the transformation between pre-change and post-change is a simple linear transformation. The idea of PCC is that vector ρ_n can be expanded by adding more terms (i.e., i_1^2, i_2^2, i_3^2, ..., i_n^2), so that better results can be achieved.

1.1. If pre-change and post-change images have only three-bands (R, G, and B):

If the pre-change and post-change images have only three bands (i.e., $b = 3$, and i_1=R, i_2=G, i_3=B), we have following polynomial kernel function ρ:

$$\rho = [R, G, B, RB, RG, BG, R^2, G^2, B^2, RGB] \quad (1)$$

1.2. If pre-change and post-change images have four or more-bands

If pre-change and post-change images have four bands (i.e., $b = 4$, and i_1=R, i_2=G, i_3=B, i_4=Y), we have following polynomial kernel function ρ:

$$\begin{aligned}\rho = [&R, G, B, Y, RG, RB, RY, GB, GY, BY,\\ &R^2, G^2, B^2, Y^2, RGB, RGY, RBY, GBY,\\ &RGBY]\end{aligned} \quad (2)$$

For pre-change and post-change images having more than four bands ($b > 4$), we consider polynomial terms up to third order to construct the kernel function considering the computational complexity of PCC.

1.3. Additional PCC results on OSCD dataset.

Figure 1, shows additional qualitative results on PCC on OSCD dataset [1]. From the figure we can observe that how well the polynomial correction transforms pre-change image color space in to the post-change color space via polynomial regression. This procedure greatly reduces the isolated colorimetric changes between pre-change and post-change images. Therefore, the resulting difference image $\mathbf{I}_d$ is less sensitive to the color shifts between pre-change and post-change images.

2. How our "Deep Metric Learning CD" algorithm converges to optimum solution

Figure 2, 3, 4, 5, 6, and 7 depict given a pre-change and post-change image pair $\{\mathbf{I}_1, \mathbf{I}_2\}$, how our proposed algorithm finds the change probability map $\mathbf{P}_c$. Our algorithm takes difference image $\mathbf{I}_d$ as input and process it through a Deep-Change Probability Generator (D-CPG) to generate the change probability map $\mathbf{P}_c$. The change probability map $\mathbf{P}_c$ is used to calculate the the proposed unsupervised loss for CD $\mathcal{L}_{\text{CD}}$. We iteratively minimize $\mathcal{L}_{\text{CD}}$ to find the optimal change probability map $\mathcal{P}_c^*$ during the optimization process. Finally, we threshold $\mathbf{P}_c^*$ with an appropriate probability value to obtain binary change map.

3. Additional Qualitative Results on OSCD dataset

Figure 8, 9, 10, and 7 shows the final change probability map (i.e., difference image) correspond to different SOTA methods on OSCD dataset.

(a) Before PCC (b) After PCC

Figure 1. Additional qualitative examples on OSCD dataset [1] to illustrate how PCC maps pre-change image color space to post-change image color space using polynomial regression.

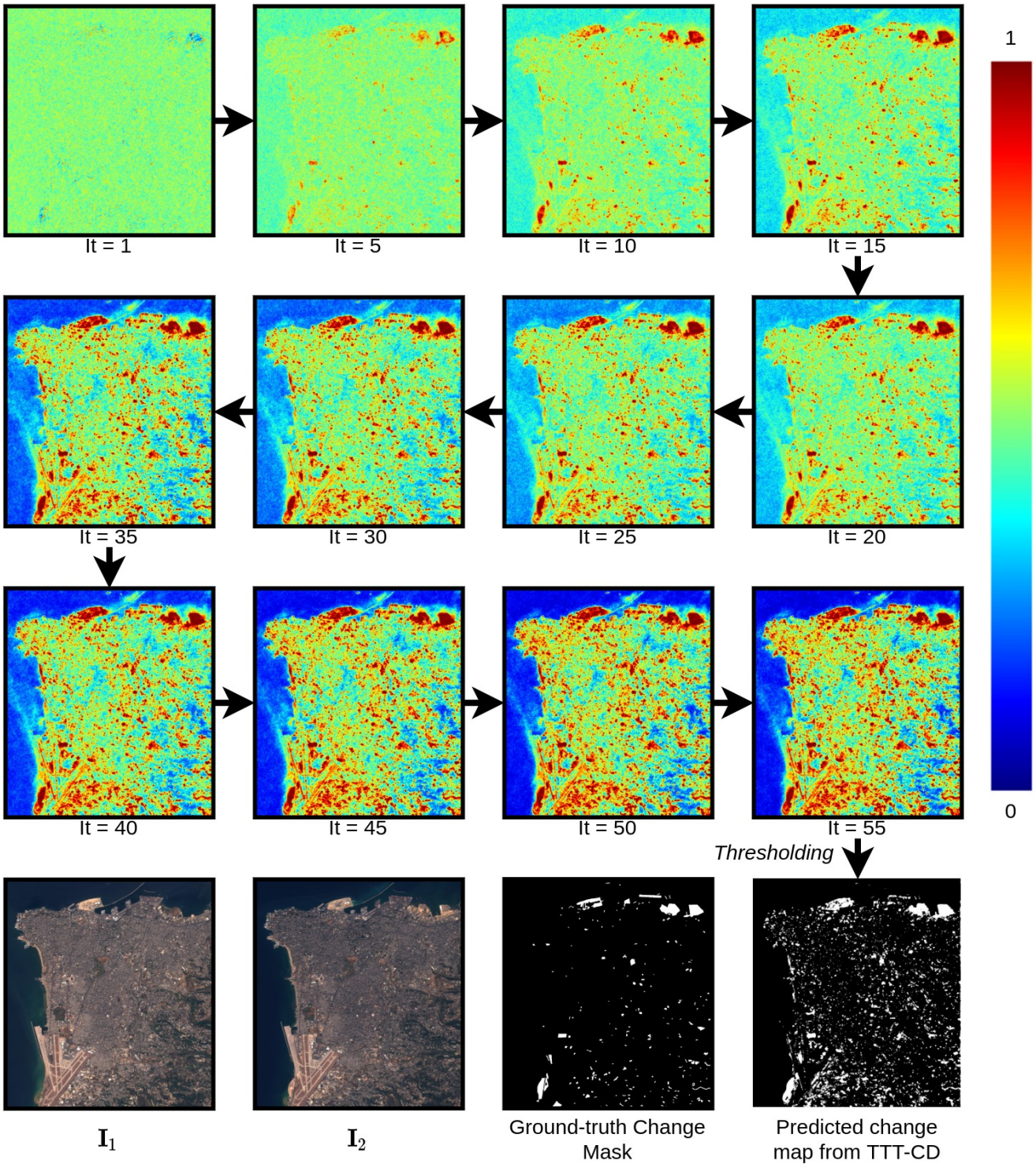

Figure 2. An example on “beirut” image in OSCD dataset.

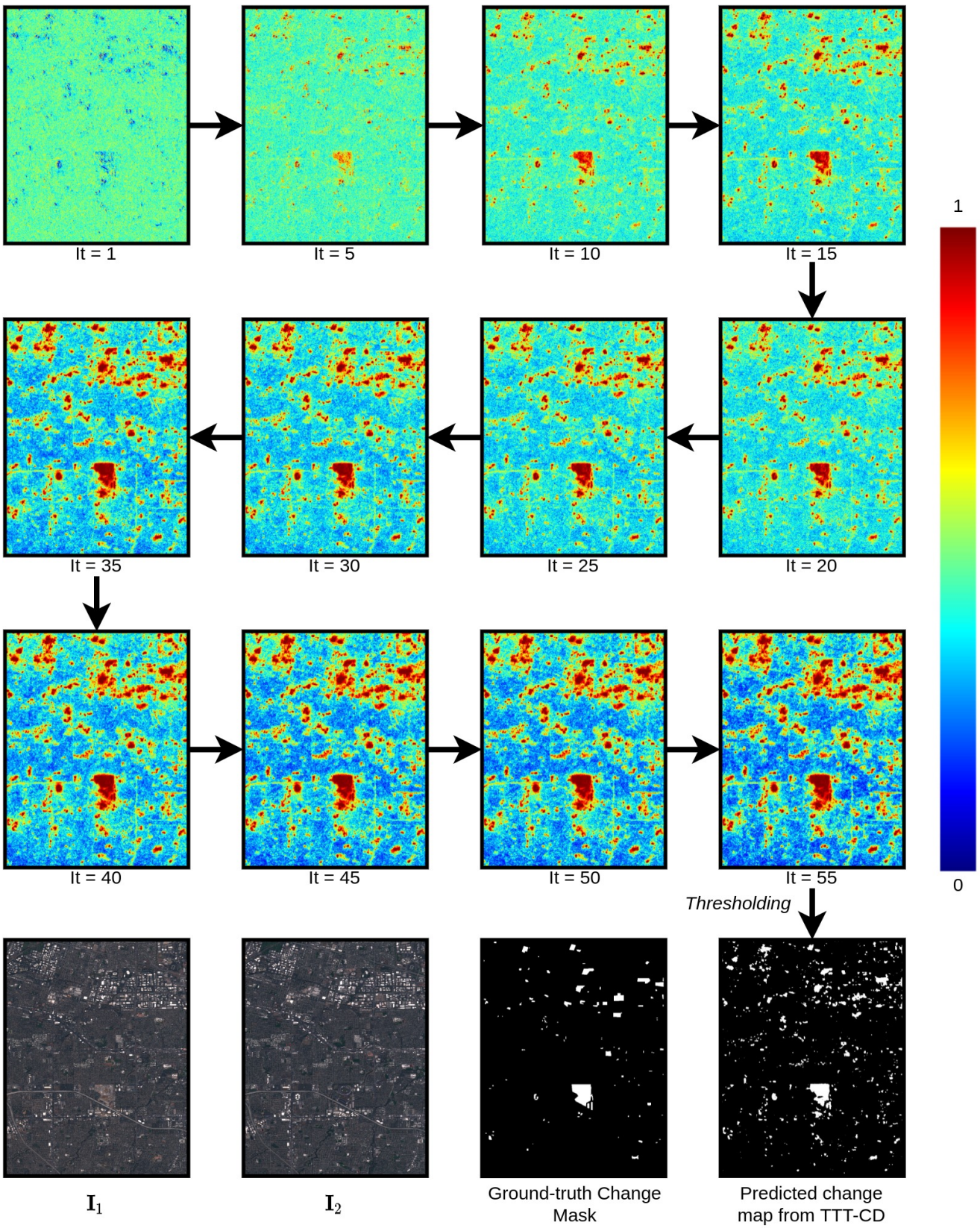

Figure 3. An example on "cupertino" image in OSCD dataset.

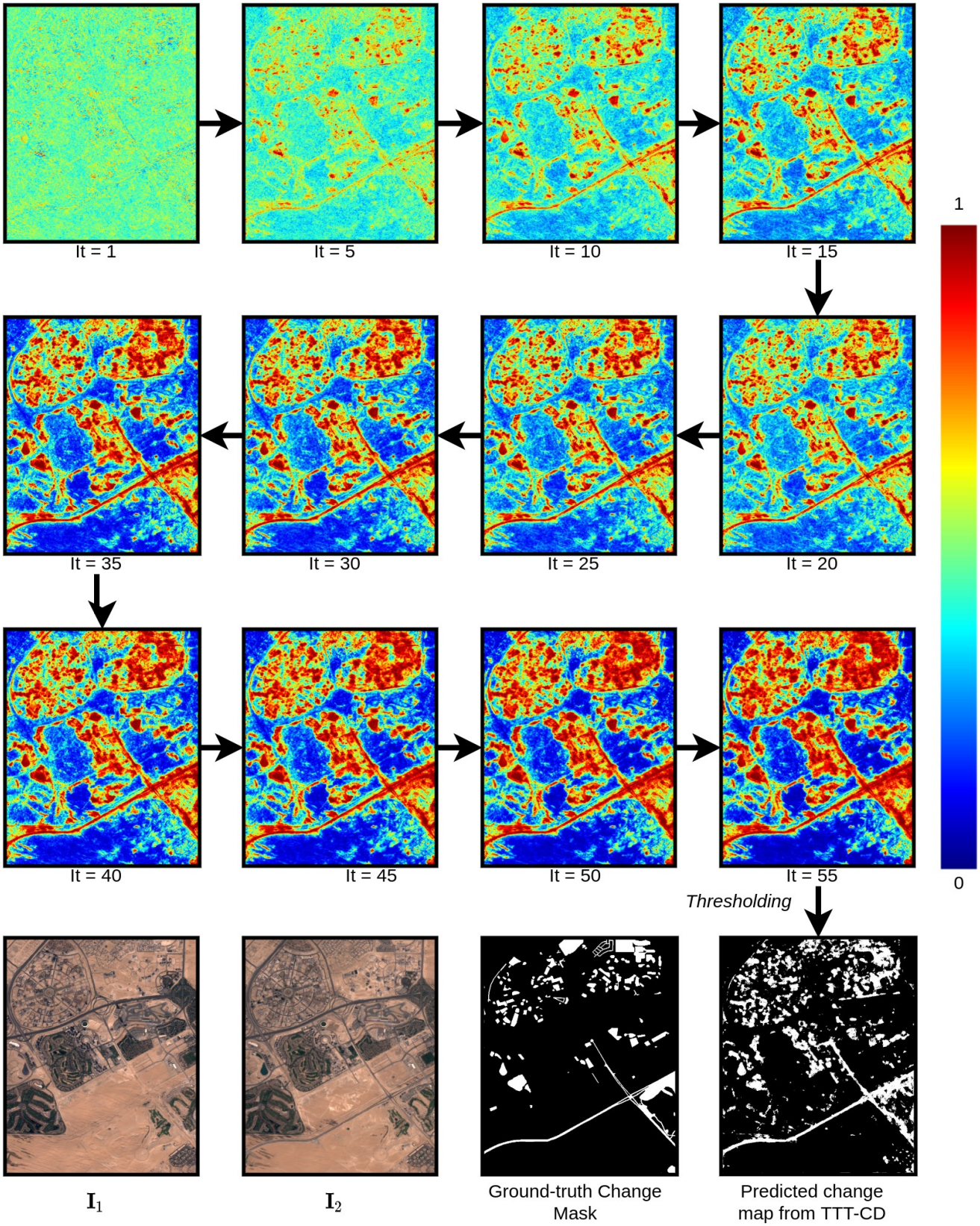

Figure 4. An example on "cupertino" image in OSCD dataset.

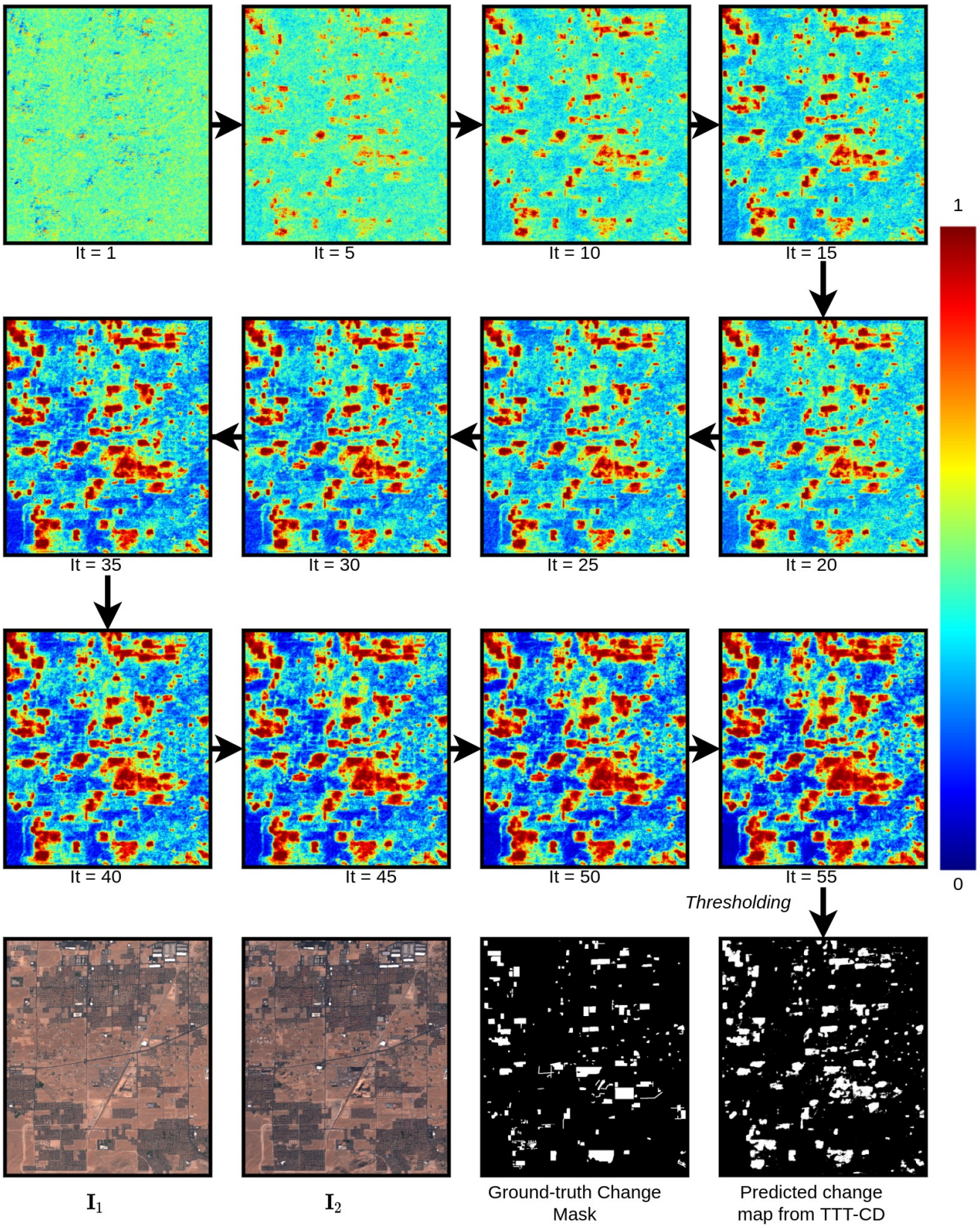

Figure 5. An example on "lasvegas" image in OSCD dataset.

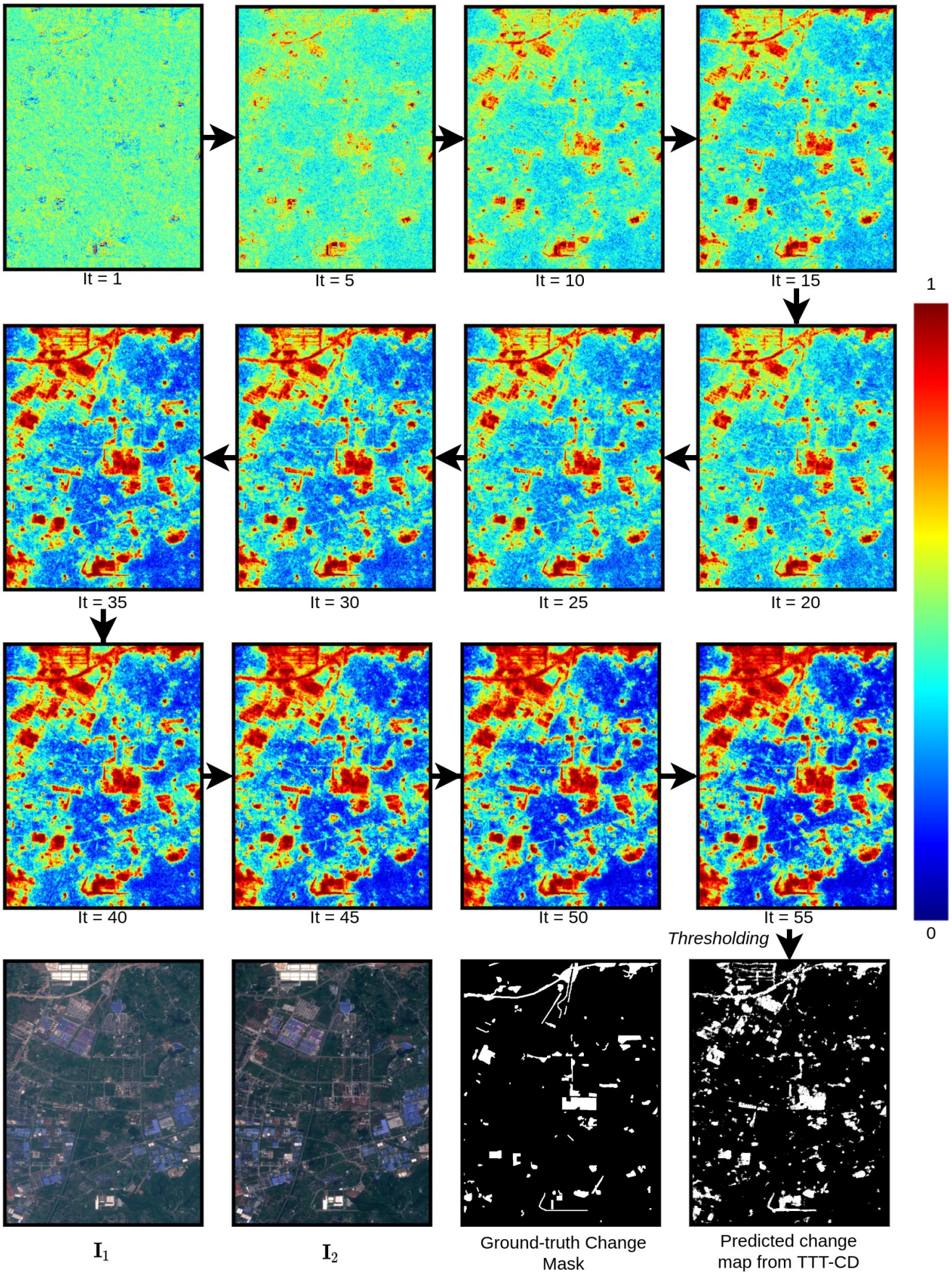

Figure 6. An example on "lasvegas" image in OSCD dataset.

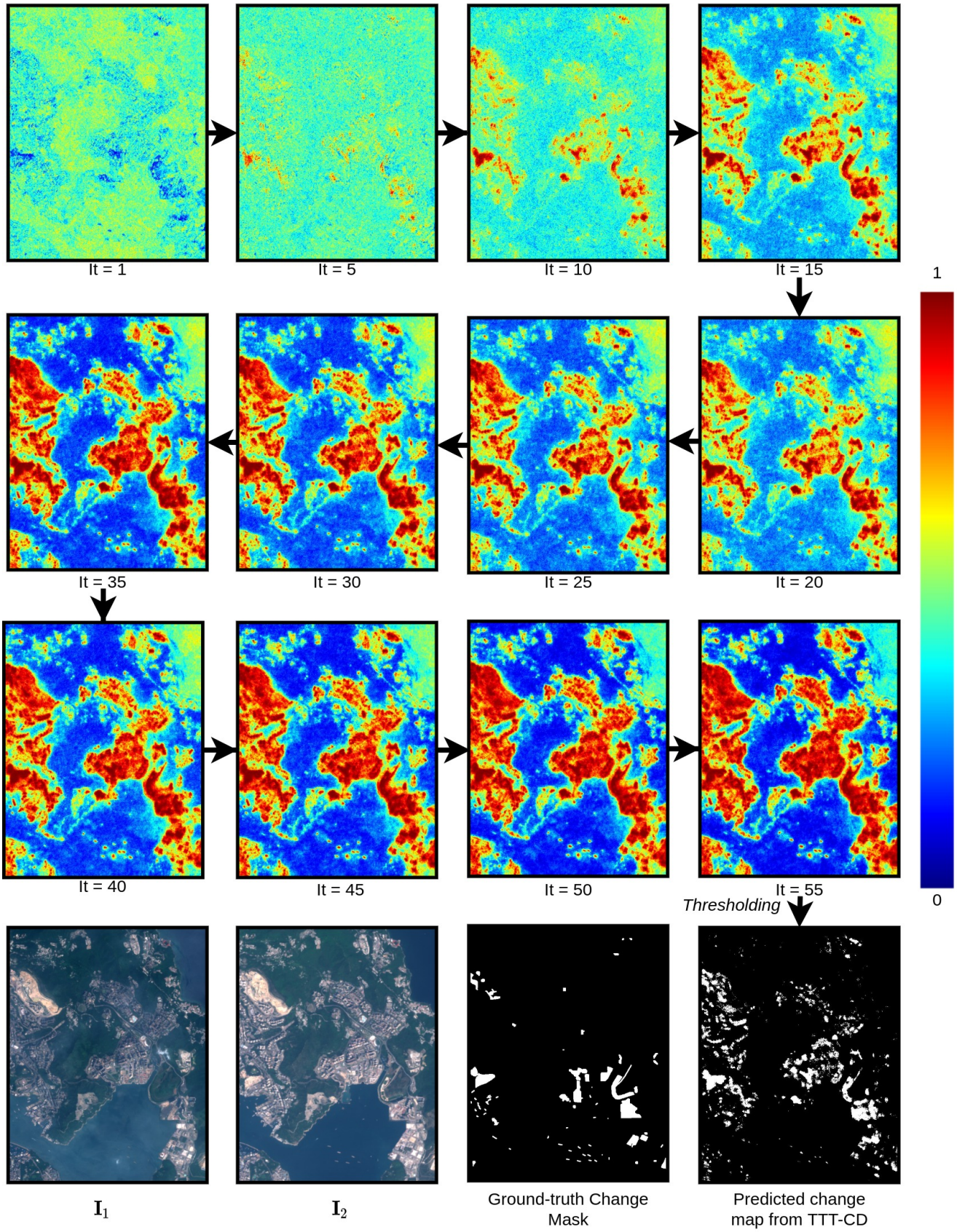

Figure 7. An example on "hongkong" image in OSCD dataset.

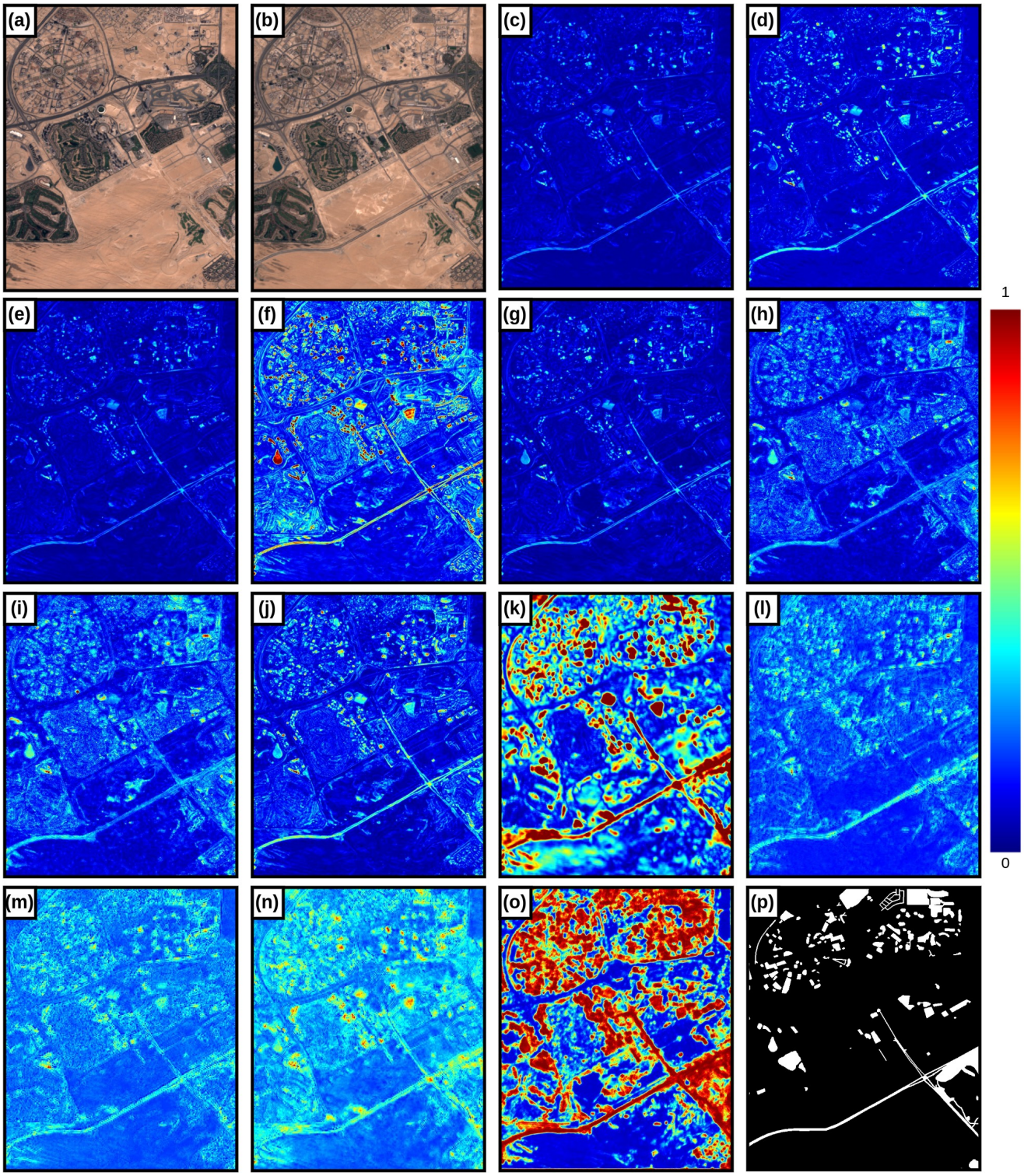

Figure 8. Change probability map (i.e., difference image) of different CD methods for dubai image pair in OSCD dataset. (a) Pre-change image. (b) Post-change image. (c) CVA. (d) DPCA. (e) ImageDiff. (f) ImageRatio. (g) ImageRegr. (h) IRMAD. (i) MAD. (j) PCDA. (k) DeepCVA. (l) UNet. (m) SeCo-Rand. (n) SeCo-Pre. (o) "Deep metric leanring CD" (ours). (p) Groud-truth change mask.

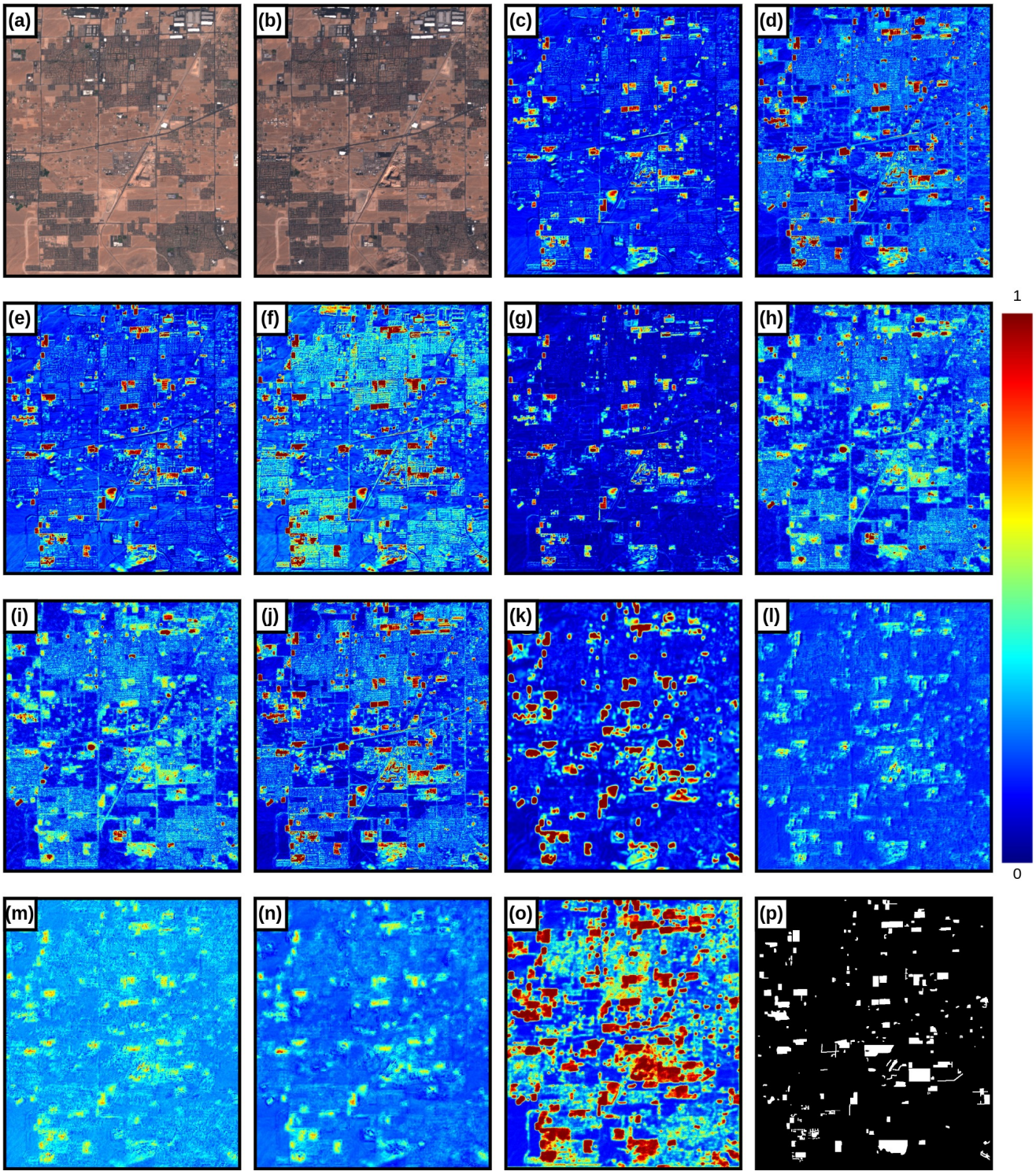

Figure 9. Change probability map (i.e., difference image) of different CD methods for lasvegas image pair in OSCD dataset. (a) Pre-change image. (b) Post-change image. (c) CVA. (d) DPCA. (e) ImageDiff. (f) ImageRatio. (g) ImageRegr. (h) IRMAD. (i) MAD. (j) PCDA. (k) DeepCVA. (l) UNet. (m) SeCo-Rand. (n) SeCo-Pre. (o) "Deep metric leanring CD" (ours). (p) Groud-truth change mask.

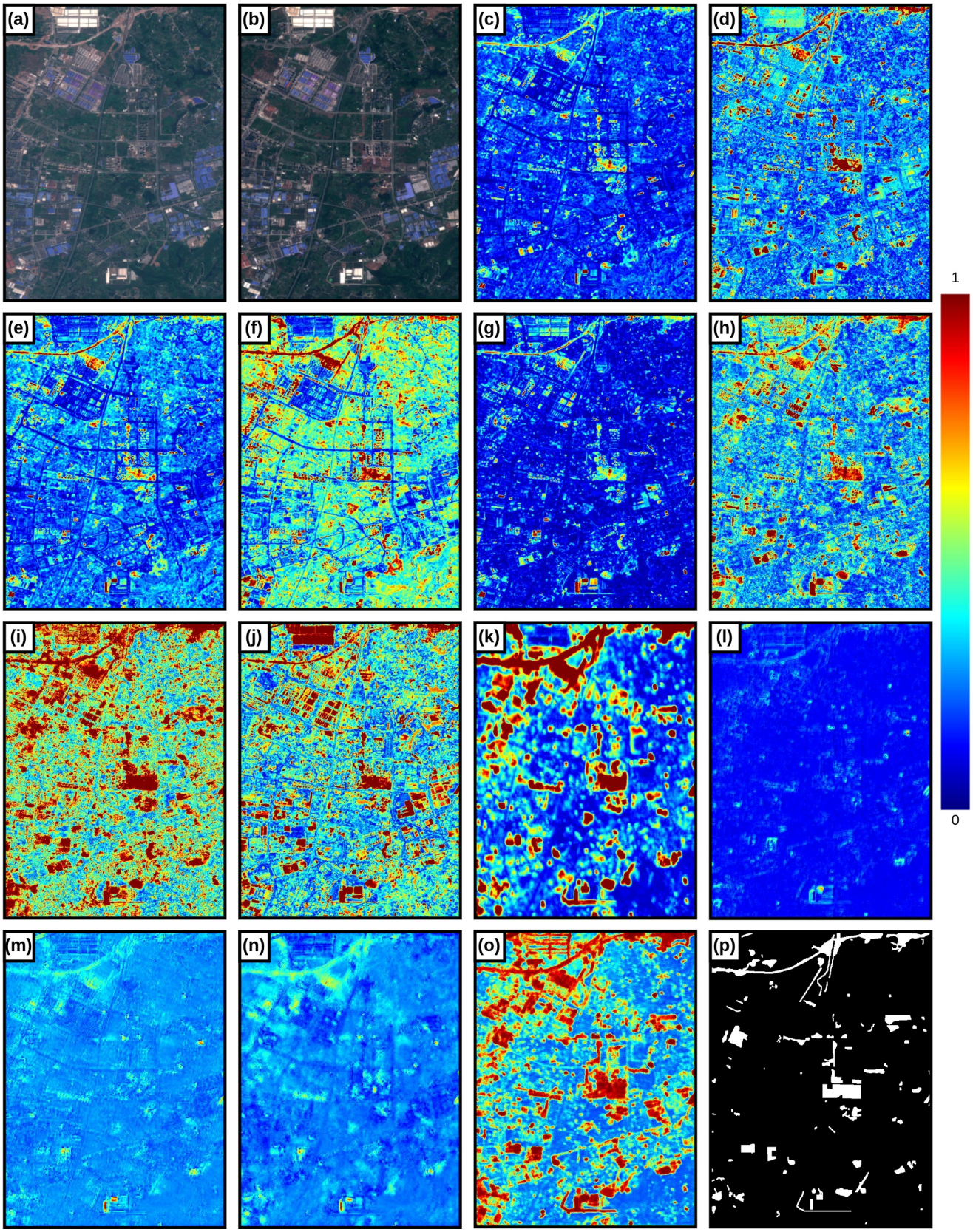

Figure 10. Change probability map (i.e., difference image) of different CD methods for chongqing image pair in OSCD dataset. (a) Pre-change image. (b) Post-change image. (c) CVA. (d) DPCA. (e) ImageDiff. (f) ImageRatio. (g) ImageRegr. (h) IRMAD. (i) MAD. (j) PCDA. (k) DeepCVA. (l) UNet. (m) SeCo-Rand. (n) SeCo-Pre. (o) "Deep metric leanring CD" (ours). (p) Groud-truth change mask.

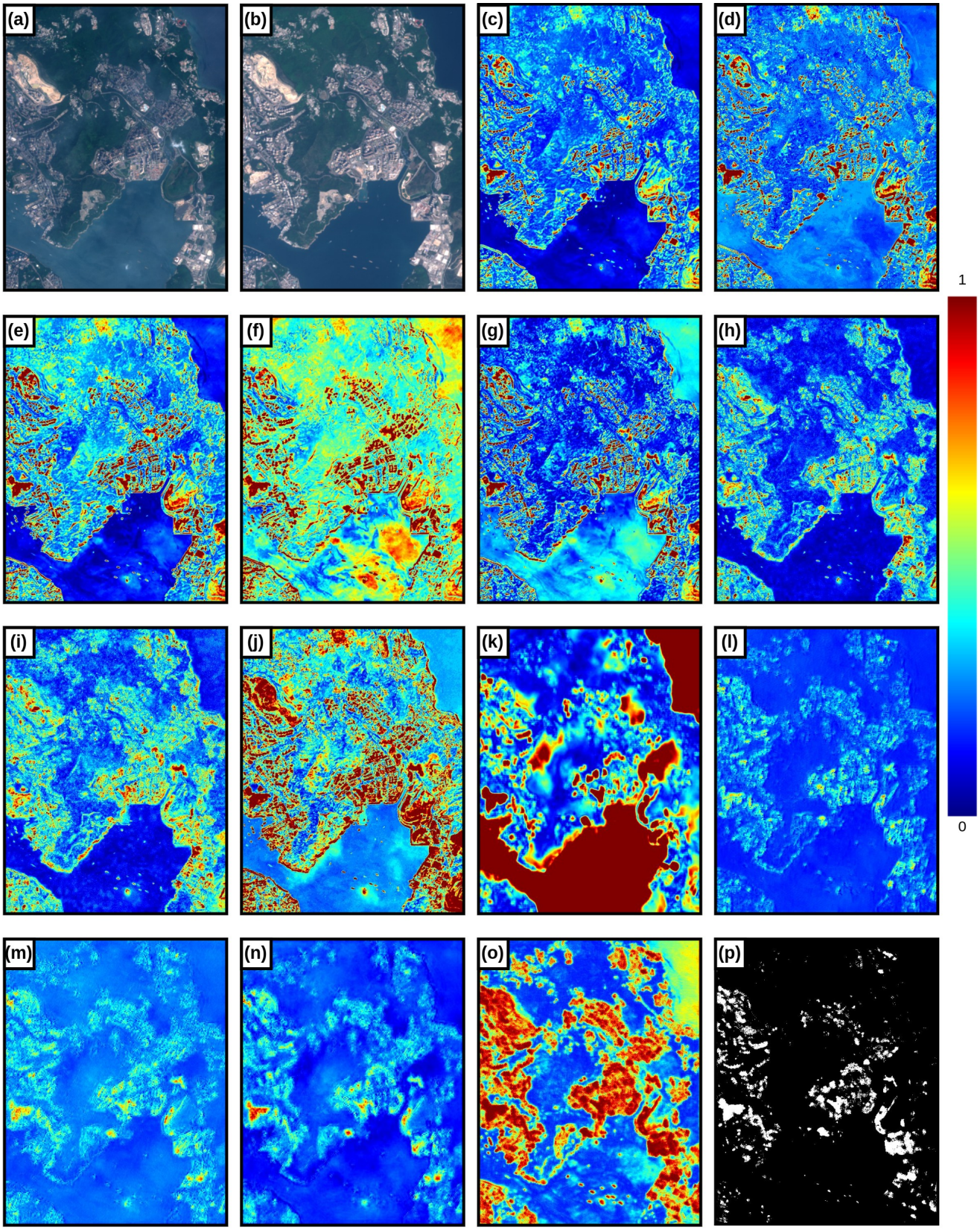

Figure 11. Change probability map (i.e., difference image) of different CD methods for hongkong image pair in OSCD dataset. (a) Pre-change image. (b) Post-change image. (c) CVA. (d) DPCA. (e) ImageDiff. (f) ImageRatio. (g) ImageRegr. (h) IRMAD. (i) MAD. (j) PCDA. (k) DeepCVA. (l) UNet. (m) SeCo-Rand. (n) SeCo-Pre. (o) "Deep metric leanring CD" (ours). (p) Groud-truth change mask.

4. Limitations and Future Work

Since the proposed TTT-CD approach optimizes network parameters for each MT-RSI separately at test-time to estimate the change probability map, the inference time (testing time) of the proposed method is higher when compared with SOTA supervised, self-supervised, and unsupervised methods. For example, the average inference time of a supervised method: SeCo [2], and an unsupervised method: D-CVA [3] are about 1.9 s and 8.2 s for an MT-RSI with a spatial resolution of 1154×740, respectively. In comparison, the proposed method takes about 18.4 s to iteratively estimate the change probability map of the same test MT-RSI. We will address this limitation of the proposed TTT-CD in our future work.

References

[1] Caye Daudt, R., Le Saux, B., Boulch, A., Gousseau, Y.: Urban change detection for multispectral earth observation using convolutional neural networks. In: IEEE International Geoscience and Remote Sensing Symposium (IGARSS) (July 2018) 1, 2

[2] Mañas, O., Lacoste, A., Giro-i Nieto, X., Vazquez, D., Rodriguez, P.: Seasonal contrast: Unsupervised pre-training from uncurated remote sensing data. arXiv preprint arXiv:2103.16607 (2021) 13

[3] Saha, S., Bovolo, F., Bruzzone, L.: Unsupervised deep change vector analysis for multiple-change detection in vhr images. IEEE Transactions on Geoscience and Remote Sensing **57**(6), 3677–3693 (2019). https://doi.org/10.1109/TGRS.2018.2886643 13